74574_Auto_Edited - check.docx

Radiomics for differentiating tumor deposits from lymph node metastasis in rectal cancer

Zhang YC et al Radiomics for identifying TDs

Yong-Chang Zhang, Mou Li, Yu-Mei Jin, Jing-Xu Xu, Chen-Cui Huang, Bin Song

Abstract

BACKGROUND

Tumor deposits (TDs) are not equivalent to lymph node (LN) metastasis (LNM) but have become independent adverse prognostic factors in patients with rectal cancer (RC). Although preoperatively differentiating TDs and LNMs is helpful in designing individualized treatment strategies and achieving improved prognoses, it is a challenging task.

AIM

To establish a computed tomography (CT)-based radiomics model for preoperatively differentiating TDs from LNM in patients with RC.

METHODS

This study retrospectively enrolled 219 patients with RC [TDs+LNM- (n = 89); LNM+ TDs- (n = 115); TDs+LNM+ (n = 15)] from a single center between September 2016 and September 2021. Single-positive patients (i.e., TDs+LNM- and LNM+TDs-) were classified into the training (n = 163) and validation (n = 41) sets. We extracted numerous features from the enhanced CT (region 1: The main tumor; region 2: The largest peritumoral nodule). After deleting redundant features, three feature selection methods and three machine learning methods were used to select the best-performing classifier as the

radiomics model (Rad-score). After validating Rad-score, its performance was further evaluated in the field of diagnosing double-positive patients (*i.e.*, TDs⁺LNM⁺) by outlining all peritumoral nodules with diameter (short-axis) > 3 mm.

RESULTS

Rad-score 1 (radiomics signature of the main tumor) had an area under the curve (AUC) of 0.768 on the training dataset and 0.700 on the validation dataset. Rad-score 2 (radiomics signature of the largest peritumoral nodule) had a higher AUC (training set: 0.940; validation set: 0.918) than Rad-score 1. Clinical factors, including age, gender, location of RC, tumor markers, and radiological features of the largest peritumoral nodule, were excluded by logistic regression. Thus, the combined model was comprised of Rad-scores of 1 and 2. Considering that the combined model had similar AUC with Rad-score 2 (P = 0.134 in the training set and 0.594 in the validation set), Rad-score 2 was used as the final model. For the diagnosis of double-positive patients in the mixed group [TDs+LNM+ (n = 15); single-positive (n = 15)], Rad-score 2 demonstrated moderate performance (sensitivity, 73.3%; specificity, 66.6%; and accuracy, 70.0%).

CONCLUSION

Radiomics analysis based on the largest peritumoral nodule can be helpful in preoperatively differentiating between TDs and LNM.

Key Words: Radiomics; Tumor deposits; Lymph node metastasis; Rectal cancer; Computed tomography; Differential diagnosis

Zhang YC, Li M, Jin YM, Xu JX, Huang CC, Song B. Radiomics for differentiating tumor deposits from lymph node metastasis in rectal cancer. *World J Gastroenterol* 2022; In press

Core Tip: In this study, a radiomics model based on the largest peritumoral nodule was developed to preoperatively differentiate tumor deposits (TDs) from lymph node (LN) metastasis in patients with rectal cancer. This model demonstrated good performance in both the training and validation cohorts. However, its performance decreased with the diagnosis of the double-positive patients. In summary, this model can be helpful for differentiating TDs from LN metastases.

13 INTRODUCTION

Colorectal cancer (CRC) ranks third in terms of incidence and second in terms of mortality^[1], and RC accounts for approximately 30% of CRC^[2]. Tumor deposits (TDs) in RC are defined as discontinuous extramural extensions or focal aggregates of adenocarcinoma located in the perirectal region, vascular/neural structures^[3,4]. As a factor for poor prognosis, TDs have attracted widespread attention in recent years^[4,5]. A review published in 2017 confirmed that TDs were independently associated with lower overall and disease-free survival according to data available in the literature^[4].

Clearly, TDs are not equivalent to LN metastasis (LNM) in terms of biology and prognosis. Among patients with LNM, the occurrence of TDs can lead to a worse prognosis^[4,5], strongly indicating that their impact on prognosis is independent and additive. Therefore, TDs must be reported separately from LNM^[6]. However, TDs and LNM can only be determined through pathological examinations of surgical specimens^[7]. Presently, it is difficult to

preoperatively differentiate TDs from LNM using computed tomography (CT).

Radiomics is a rapidly developing field of research that involves the extraction of numerous quantitative features from medical images. These features can capture characteristics of volume of interest (VOI), such as heterogeneity, and it may, alone or in combination with other data, be used to solve clinical problems^[8]. Recently, some studies have reported the involvement of TDs in RC^[6,9,10]. However, some previous studies did not focus on the differentiation of TDs from LNM^[9,10], and Atre *et al*^[6] used only texture analysis and lacked the construction and validation of a model.

Therefore, we aimed to establish a CT-based radiomics model to preoperatively differentiate TDs from LNM in patients with RC.

MATERIALS AND METHODS

Patients

This retrospective study was approved by the institutional review board (No. 1159) of the authors' hospital. Given the retrospective design and use of anonymized patient data, requirements for informed consent were waived.

Patient data collected between September 2016 and September 2021 were reviewed by searching radiological and pathological databases. A total of 219 patients [single-positive, 112 male, 92 female; mean \pm SD age, 60 \pm 12 years (range, 32-92 years); double-positive, 6 male, 9 female; mean age, 60 \pm 13 years (range, 37-83 years)] were enrolled. The inclusion criteria were as follows: Diagnosis of rectal adenocarcinoma on pathology; single positive result (*i.e.*, TDs+ or LNM+); and 15 randomly selected patients who were TDs+LNM+. The exclusion criteria were as follows: No peritumoral nodules with short-axis diameter > 3 mm on enhanced CT images (n = 22); incomplete clinical data, such as tumor markers (n = 36); patients who did not undergo surgery (n = 5);

treatment before CT examination (n = 2); and poor-quality CT images (n = 4). Figure 1 shows the flow diagram of patient recruitment. Figure 2 shows the workflow of this radiomics study. Clinical characteristics, including age, gender, location of RC, tumor markers, pTN stage, extramural vascular invasion (EMVI), histological grade, and radiological features of the largest peritumoral nodule, are summarized in Table 1.

Reference standard

Pathological confirmation reports based on surgically resected specimens were obtained from the hospital's electronic medical database. From these reports, pathological information about the main tumor and peritumoral nodules (status and number of TDs and LNMs) were obtained.

Image acquisition and evaluation

Chest-abdomen-pelvis enhanced CT can detect not only the primary tumor but also suspected metastases. The main scanning parameters of CT are described in the Supplementary Table 1.

Two experiential radiologists reviewed the CT images and recorded the radiological features while blinded to clinical and pathological information. As shown in Table 1, the tumor location and radiological features of the largest peritumoral nodule, such as size, morphology, spiculation, and CT value, was confirmed by summarizing the results of these two radiologists (disagreements were resolved by consensus discussion).

Feature extraction and model-building

The reliability of the radiomics features was tested in twenty patients. The features with intra-/inter-class correlation coefficients (ICCs) > 0.75 were considered stable^[11]. Thereafter, the radiologists independently segmented

the main tumor and largest peritumoral nodule by manually drawing three-dimensional VOI (Figure 2). All images were resampled to pixel spacing of 1 mm in all three dimensions. Several transformation methods, such as wavelet filter and Laplace of Gaussian filter, were applied to the original images. PyRadiomics was used to extract features from the original and filtered images^[12]. Figure 2 shows the types of the features. The correlation analysis was performed to remove redundant features. In detail, if the correlation coefficient between two features was > 0.4, the one with a lower coefficient was removed. Subsequently, three feature selection methods and three machine learning methods were tested to select the best performing classifier as the radiomics model (*i.e.*, Rad-score). Statistically significant factors from univariate and multivariate logistic regression analyses were used to develop the combined model.

Model evaluation

Receiver operating characteristic (ROC) curves of the models were performed to assess and compare their performance in identifying TDs+LNM⁻ patients. Moreover, the performance of the models in diagnosing double-positive (*i.e.*, TDs+LNM⁺) patients were further evaluated by outlining all peritumoral nodules with short-axis diameters > 3 mm in the mixed group [TDs+LNM⁺ (n = 15); randomly selected single-positive patients from the training or validation sets (n = 15)]. If there were two different results (TD⁺ or LNM⁺) in all the outlined peritumoral nodules of each patient, double-positive patients were considered to be diagnosed correctly.

¹⁸ Statistical analysis

Statistical analyses were performed using SPSS (IBM Corporation, Armonk, NY, United States), Stata (StataCorp LP, College Station, TX, United States),

and MedCalc software. In Table 1, continuous variables were analyzed using *t*-test or Mann-Whitney *U* test, and categorical variables were compared using the chi-squared test or Fisher's exact test. The areas under the curve (AUCs) of the models were compared using DeLong's test.

RESULTS

Patient characteristics

A total of 219 patients with RC [TDs+LNM- (n = 89); LNM+TDs- (n = 115); TDs+LNM+ (n = 15)] were enrolled in this study. Clinical factors, including pathological N stage, pathological EMVI, and the size and shape of the largest peritumoral nodule, were found significantly different between the TDs+LNM- group and LNM+TDs- group. No statistical differences were found in age, gender, location of RC, tumor markers, pathological T stage, histological grade, and other features of the peritumoral nodule (spiculation and CT values) between the TDs+LNM- group and LNM+TDs- group. The patients were classified into a training set (n = 163) and a validation set (n = 163). Except for carcinoembryonic antigen (n = 163) and a validation differences were found in the other clinical factors between the training and validation sets (Table 1).

Feature selection and model building

After evaluating the reliability, a large number of radiomics features remained (n = 1490 extracted from the tumor and 1252 from the largest peritumoral nodule), with ICCs of > 0.75. After excluding redundant radiomics features, we selected features using the 11-based method and established Rad-score using a logistic regression analysis. Features included in Rad-score are reported in the Supplementary Tables 2 and 3. Rad-score of the main tumor (Rad-score 1) and that of the largest peritumoral nodule (Rad-score)

score 2) were independent risk factors for differentiating TDs from LNM [odds ratio (OR) = 3.267 and 14.396, respectively]. Regarding clinical factors, although the size and shape of the largest peritumoral nodule had significant difference between the TDs⁺ group and LNM⁺ group, they were all deleted in the logistic regression (P = 0.314 and 0.948, respectively; Table 2). Furthermore, a combined model integrating Rad-scores of 1 and 2 was established using the logistic regression.

Model evaluation

For classification results, the AUC for Rad-score 1 was 0.768 [95% confidence interval (CI): 0.695-0.830] in the training set and 0.700 (95%CI: 0.537-0.833) in the validation set. Rad-score 2 achieved improved performance, with an AUC of 0.940 (95%CI: 0.892-0.971) in the training set and 0.918 (95%CI: 0.789-0.981) in the validation set. The combined model (Rad-scores 1 + 2) had similar AUCs to Rad-score 2 in both the training and validation sets, as shown in Table 3 and Figure 3. Thus, Rad-score 2 (Rad-score of the largest peritumoral nodule) was used as the final model owing to its simplicity.

In the calibration curve for Rad-score 2, the solid line was close to the reference line (dotted line), indicating that Rad-score 2 demonstrated good agreement between the prediction (x-axis) and observation (y-axis) (Figure 4). However, Rad-score 2 still overestimated the actual risk for TDs+ (approximately 10%, at most). A decision curve was constructed to evaluate the clinical utility of Rad-score 2 in differentiating TDs from LNM. The net benefit can be measured along the y-axis. Figure 4 shows that Rad-score 2 yielded thore benefit than "treat all," "treat none," and Rad-score 1. A case example is shown in Figure 5.

Moreover, all peritumoral nodules with short-axis diameter > 3 mm were delineated in each patient in the mixed group [TDs+LNM+ (n = 15); single-

positive (n = 15)] to evaluate the performance of the models in predicting double-positive (i.e., TDs⁺LNM⁺) patients. Of the 30 patients, 134 peritumoral nodules were delineated. Rad-score 2 had a moderate accuracy of 70% (sensitivity, 73.3%; specificity, 66.6%). Because the combined model had the same accuracy of 70% as Rad-score 2, it confirmed the use of Rad-score 2 as the final model.

Subgroup analysis

In view of the prognostic difference between the upper and middle-lower RC^[13], we performed a subgroup analysis indicating that Rad-score 2 had high AUCs in both the upper [0.941 (95%CI: 0.853-0.984)] and middle-lower [0.931 (95%CI: 0.875-0.967)] RC groups. For patients receiving neoadjuvant chemoradiotherapy (nCRT), Rad-score 2 also had high AUCs, as shown in Table 4. In these subgroup analyses, Rad-score 2 outperformed Rad-score 1.

The American Joint Committee on Cancer (AJCC) tumor-node-metastasis (TNM) staging system has not correlated a higher number of TDs with staging, unlike LNs (*e.g.*, N1, 1-3 and N2, \geq 4 regional LNs)^[14]. Several authors have found that patients with \geq 3 TDs have a significantly worse prognosis than those with 1-2 TDs^[15]. However, in this study, the values of Rad-scores 1 and 2 were not significantly different between the \geq 3 TDs group and the 1-2 TDs group (P = 0.838 for Rad-score 1, and P = 0.309 for Rad-score 2) (Table 4).

DISCUSSION

Our study established a new radiomics signature (Rad-score 2) based on 11 features extracted from the largest peritumoral nodule, demonstrating the potential for preoperatively differentiating TDs from LNM. Moreover, Rad-score 2 outperformed Rad-score 1 (based on the main tumor) in this field

[0.918 vs 0.700 (P = 0.032) in the validation set]. However, this model had a minor overestimation of TDs⁺ probability for most of the included patients.

The 8th AJCC TNM staging system incorporates a N1c category for RC patients with TDs+LNM⁻. The N1c category represents 5% to 10% of RC with TDs (TDs+LNM- and TDs+LNM+) observed in approximately 20% of all rectal adenocarcinomas^[5]. Although many authors have speculated on the origin of TDs, the phenomenon remains unclear. However, some authors have found that a significant proportion of TDs cannot be traced back to the LN^[16]. Goldstein *et al*^[17] reported that, after performing experiments on deeper sections, most TDs (up to 90%) exhibited signs of > 1 origin. Currently, the only method to determine the status of peritumoral nodules is the histopathologic examination of the resected specimens. The preoperative differentiation of TDs and LNM facilitates the design of individualized treatment strategies and evaluation of prognosis.

Unlike CT and magnetic resonance imaging (MRI), radiomics may solve clinical problems by extracting an enormous number of features which can quantify invisible differences in tissues for the human eye. Several radiomics studies investigating TDs^[6,9,10] and LNM^[18-21] have been reported in RC. There were, however, some differences in our study. First, in contrast to most previous models (predicting single factor positive TDs^[9,10] or LNM^[18-21]), our model can be used to predict the status of both TDs and LNM. When a peritumoral nodule with a short-axis diameter > 3 mm was found on CT images, we could then use our model to predict the classification of this nodule (TDs⁺ or LNM⁺) and further identify the patient as TDs⁺ only, LNM⁺ only, or double positive. Second, we delineated the main tumor and the largest peritumoral nodule, while previous authors delineated the tumor and whole peritumoral fat^[10] or only the main tumor^[9]. Third, our study included a larger sample size of TDs⁺ patients (*n* = 89) and had a higher AUC (0.918 in

the validation set) than those reported by Chen *et al*^[10] [TDs⁺ (n = 40); AUC 0.795], Yang *et al*^[9] [TDs⁺ (n = 23); AUC 0.820], and Atre *et al*^[6] [TDs⁺ (n = 25); AUC 0.810]. Finally, although Atre *et al*^[6] could also predict both TDs⁺ and LNM⁺, they only performed texture analysis, which was clearly different from the analysis in our study.

Notably, double-positive patients had a worse prognosis than those with TDs+ or LNM+ only. One positive LN 5-year survival rate was 62% without TDs, vs 44% with TDs[4]. Thus, preoperative diagnosis of double-positive patients is of great clinical significance. However, the performance of the model decreased (accuracy, 70%) when used to diagnose double-positive patients. We speculated that this may be related to the following factors. First, we established a model based on the largest peritumoral nodule. When diagnosing double-positive patients, we used all peritumoral nodules (> 3 mm). Thus, the mean size in the mixed group was smaller than that in the training set. Second, the sample size of the mixed group was small. Third, among the double-positive patients, some LNMs were incorrectly evaluated as TDs. In these lesions, the value of wavelet-HLH_firstorder_Median (a radiomics feature) decreased. In the future, we will include a larger sample to improve the applicability of the model in double-positive patients.

Nevertheless, the nature of TDs after neoadjuvant therapy remains unclear. Regarding the 77 patients who underwent nCRT in our study, the AUC for the Rad-score 2 did not decrease significantly (0.897), indicating that the model was stable. Regarding the tumor location, the AUCs of the model were also similar between the upper and middle-lower RC. Our model failed to differentiate between groups with \geq 3 TDs and 1-2 TDs (P = 0.309).

Our study had several limitations. Firstly, because this was a retrospective study, selection bias may have been introduced. Secondly, to directly compare peritumoral nodules, we especially selected a sample comprising TDs+LNM-

and LNM+TDs- and outlined the largest peritumoral nodule. However, it was still possible to identify benign peritumoral nodules. Thirdly, this was a single-center analysis. In the future, it will be necessary to conduct an external validation to confirm the versatility of the model.

CONCLUSION

A radiomics signature based on the largest peritumoral nodule is established in this article. This signature can facilitate the preoperative differentiation of TDs from LNM.

ARTICLE HIGHLIGHTS

Research background

Tumor deposits (TDs) are not equivalent to lymph node (LN) metastasis (LNM) but have become independent adverse prognostic factors in patients with rectal cancer (RC). If TDs can be differentiated from LNM before therapy, individualized treatment and patient prognosis may greatly improve.

Research motivation

Currently, preoperative differentiation of TDs and LNM can be challenging.

Research objectives

To establish a radiomics model for preoperatively differentiating between TDs and LNM in patients with RC.

Research methods

The present study retrospectively enrolled 219 patients with RC [TDs+LNM-(n = 89); LNM+TDs-(n = 115); TDs+LNM+(n = 15)] from a single center

between September 2016 and September 2021. Single-positive patients (TDs⁺LNM⁻ and LNM⁺TDs⁻) were classified into training (n = 163) and validation (n = 41) sets. Rad-scores were established based on the main tumor and largest peritumoral nodule. After validating Rad-score, we further evaluated its performance for diagnosing double-positive patients (*i.e.*, TDs⁺LNM⁺) by outlining all peritumoral nodules with diameters > 3 mm (short axis).

Research results

Rad-score 1 (radiomics signature of the main tumor) had an area under the curve (AUC) of 0.768 on the training dataset and 0.700 on the validation dataset. Rad-score 2 (radiomics signature of the largest peritumoral nodule) had a higher AUC (training set: 0.940; validation set: 0.918) than Rad-score 1. For the diagnosis of double-positive patients in the mixed group [TDs+LNM+ (n = 15); single-positive (n = 15)], Rad-score 2 demonstrated moderate performance (sensitivity, 73.3%; specificity, 66.6%; and accuracy, 70%).

Research conclusions

The radiomics signature of the largest peritumoral nodule could provide individualized preoperative differentiation of TDs and LNM. Moreover, it was helpful in diagnosing patients who were TDs⁺LNM⁺.

Research perspectives

To improve the model, surgeons, radiologists, and pathologists should collaborate through prospective research to achieve node-to-node correspondence between CT images and pathological examinations in the future.

5 Figure Legends

Figure 1 Flowchart of patients' recruitment pathway. RC: Rectal cancer; CT: Computed tomography; TDs: Tumor deposits; LNM: Lymph node metastasis.

Figure 2 Radiomics workflow. 3D VOI: Three-dimensional volume of interest; GLCM: Gray level co-occurrence matrix; GLSZM: Gray level size zone matrix; GLRLM: Gray level run length matrix; GLDM: Gray level dependence matrix; NGTDM: Neighbouring gray tone difference matrix; ROC: Receiver operating characteristic curve.

Figure 3 Comparisons of the receiver operating characteristic curves. A: In the training set: AUC = 0.768 for Rad-score 1, 0.955 for the combined model, and 0.940 for Rad-score 2; B: In the validation set: AUC = 0.700 for Rad-score 1, 0.930 for the combined model, and 0.918 for Rad-score 2. Rad-score 1: Rad-score of the main tumor; Rad-score 2: Rad-score of the largest peritumoral nodule; AUC: Area under the curve.

Figure 4 Fit and usefulness evaluation of Rad-score 2. A: The calibration curve of Rad-score 2 shows good agreement between the predicted and observed risks in the training cohort; B: The decision curve demonstrates that Rad-score 2 obtains more benefit than "treat all", "treat none", and Rad-score 1. Rad-score of the main tumor; Rad-score 2: Rad-score of the largest peritumoral nodule; AUC: Area under the curve.

Figure 5 Case presentation. A: A 56-year-old man with upper RC, the nodule of TDs (size: 24 mm × 16 mm) had an irregular shape; B: A 44-year-old man with lower RC, the nodule of TDs (size: 14 mm × 11 mm) had a regular oval shape. It is difficult to distinguish TDs and LNM from conventional imaging findings. For these two patients, Rad-score of the largest peritumoral nodule achieved correct diagnosis (values = 0.98 and 0.97, respectively). RC: Rectal cancer; TDs: Tumor deposits; LNM: Lymph node metastasis.

ч	
2	

Table 1 Baseline and clinical characte	eristics of the in	characteristics of the included patients		9		
Characteristics	TDs+LNM-	LNM+TDs- $(n =$	P value	Training set (n	Training set (n Validation set (n	P
	(68 = u)	115)		= 163)	= 41)	value
Age (mean ± SD, yr)	59 ± 12	61 ± 12	0.268	60 ± 12	60 ± 11	0.965
Gender (man/woman)	49/40	63/52	696.0	94/69	18/23	0.113
Location (middle-low/high)	65/24	74/41	0.187	107/56	32/9	0.128
Neoadjuvant therapy $(+/-)$	34/55	43/72	906.0	62/101	15/26	0.864
CEA $(+/-)$ (positive $\geq 5 \text{ ng/mL}$)	42/47	43/72	0.159	75/88	10/31	0.012
CA19-9 (+/-) (positive ≥ 30	23/66	18/97	0.072	34/129	7/34	0.589
U/mL)						
CA125 $(+/-)$ (positive $\geq 24 \text{ U/mL}$) 13/76	13/76	14/101	0.611	21/142	6/35	0.767
pT stage (T1/T2/T3/T4)	0/9/70/10	4/12/93/6	0.063	4/17/127/15	0/4/36/1	0.894
pN stage $(1a/1b/1c/2a/2b)$	0/0/68/0/0	52/39/0/15/9	< 0.001	37/33/71/13/9	15/6/18/2/0	0.115
Histologic EMVI (+/-)	33/56	16/99	< 0.001	41/122	8/33	0.450
Histologic grade (G1/G2/G3)	1/63/25	6/26/36	0.299	0/113/50	1/26/14	0.901
Peritumoral nodule						
Shape (irregular/regular)	12/77	2/113	0.003	11/152	3/38	868.0

0.871	0.886	0.858	0.002	0.561
2/39	43	63 ± 23	0.71	0.62
7/156	54	64 ± 23	0.44	0.39
0.077	< 0.001	0.258	< 0.001	<0.001
2/113	41.2	65 ± 23	0.39	0.13
7/82	72.7	61 ± 22	0.71	68.0
Spiculation (+/-)	Size (mm²) (median)	CT value (HU)	Rad-score 1 (median)	Rad-score 2 (median)

Table 2 Univariate and multivariate logistic regression analysis

Variables	Univariate		Multivariate	
	OR	P value	OR	P value
Age	0.995	0.693	1	1
Gender	0.820	0.534	ı	1
Location	0.819	0.282	ı	1
CEA	1.546	0.171	ı	1
CA19-9	1.613	0.217	1	1
CA125	1.503	0.384	ı	ı

e
Ξ
σ
0
Ц
Έ
Ħ
0
Ξ
Ħ
.∺
H
٩
$\overline{}$

0.948	1	0.314	1	< 0.001	< 0.001
0.915	ı	0.999	ı	3.267	14.396
0.011	0.051	0.001	0.364	< 0.001	< 0.001
14.918	8.400	1.009	0.994	2.946	11.979
	(-				(
Shape	Spiculated (+/-)	Size (mm^2)	CT value (HU)	Rad-score 1	Rad-score 2

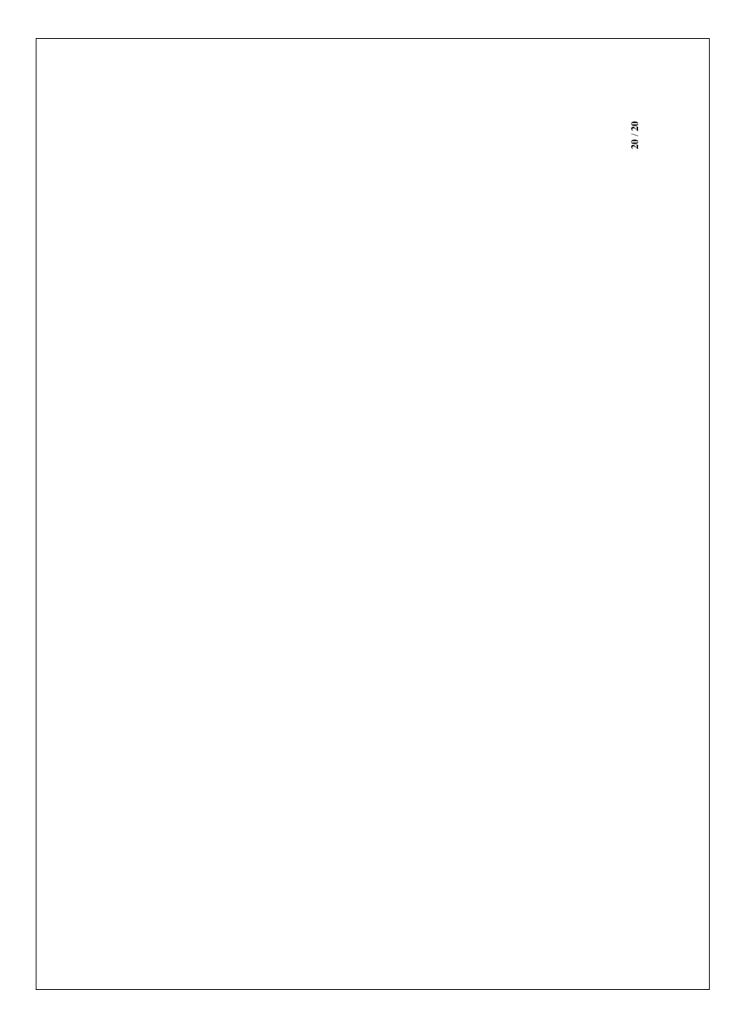
Table 3 Comparisons of the models in the training, validation, and mixed groups

	Training set	<u> </u>			Validation set	on set				Mixed group	group	
	AUC	Z	SPE	Ь	AUC		SEN	SPE	Ь	SEN	SPE	Accuracy
				value					value			
Rad-score 1	0.768 (95%CI: 0.695-	66.2%	%2'02	66.2% 70.7% < 0.001 0.700	0.700	(95%CI: 77.8% 47.8% 0.032	77.8%	47.8%	0.032			
	0.830)				0.537-0.833)	33)						
Combined	0.955 (95%CI: 0.910-	83.1%	83.1% 88.0% 0.134	0.134	0.930	(95%CI: 94.4% 82.6% 0.594	94.4%	82.6%	0.594	%9.99	73.3%	%0.02
model	0.981)				0.805-0.986)	(98						

%0.0%	
%9.99	
73.3%	
82.6%	
83.3%	
(95%CI:	(181
0.918	0.789-0.981
84.8%	
83.1%	
0.940 (95%CI: 0.892-	0.971)
Rad-score 2	

The mixed group consisted of 15 double-positive (TDs+LNM+) and 15 single-positive (11 TDs+LNM- and 4 LNM+TDs-) patients. P value: compared with Rad-score 2 by DeLong's test.

	Rad-score 1			Rad-score 2	e 2			P value
Subgroups	AUC	SEN	SPE (%)	AUC		SEN	SPE	
		(%)				(%)	(%)	
nCRT								
With $(n = 77)$	0.740 (95%CI: 0.628-	73.5%	74.4%	0.897	(95%CI:	73.5%	%2'06	0.014
	0.833)			0.806-0.954)	54)			
Without (n	= 0.753 (95%CI: 0.668- 60%	%09	86.1%	0.957	(95%CI:	89.1%	93.1%	< 0.001
127)	0.825)			0.905-0.985)	(2)			
Location								
Mid-low (n	= 0.782 (95%CI: 0.704- 75.4%	75.4%	62.2%	0.931	(95%CI: 86.2%	86.2%	82.4%	< 0.001
139)	0.848)			0.875-0.967)	(2)			
High (n = 65)	0.643 (95%CI: 0.515-	54.2%	73.2%	0.941	(95%CI:	83.3%	85.4%	< 0.001
	0.758)			0.853-0.984)	34)			
Number of TDs	1-2 (n = 50)	> 3 (n =	P =	1-2 (n = 50)	(0	= 3 (n =	P = 0.309	•
		39)	0.838			39)		
Value	0.64 ± 0.24	0.65 ±		0.83 ± 0.22	2	0.77 ±		
		0.22				92.0		



74574_Auto_Edited - check.docx

\sim	-	N I A	1 17\/	\neg	PORT
()K	1(- 1	INIΔ	1117	R-	ואווא

17% SIMILARITY INDEX

PRIMARY SOURCES

- $\frac{\text{www.frontiersin.org}}{\text{Internet}} 158 \, \text{words} 3\%$
- Mou Li, Yumei Jin, Jun Rui, Yongchang Zhang, Yali Zhao, Chencui Huang, Shengmei Liu, Bin Song. "Computed tomography-based radiomics for predicting lymphovascular invasion in rectal cancer", European Journal of Radiology, 2021 Crossref
- 3 www.ncbi.nlm.nih.gov 54 words 1 %
- www.researchsquare.com
 Internet

 46 words 1 %
- Yongchang Zhang, Zhigang Chu, Jianqun Yu, Xiaoyi Chen, Jing Liu, Jingxu Xu, Chencui Huang, Liqing Peng. "Computed tomography based radiomics for identifying pulmonary cryptococcosis mimicking lung cancer", Medical Physics, 2022 Crossref
- 6 www.jcancer.org 34 words 1%
- 5 bmcmedimaging.biomedcentral.com 31 words 1 %

- Hyeongjun Park, Donghun Lee, Sook Young Kim, Won Jae Kim. "Spontaneous Recovery of Traumatic Unilateral Superior Oblique Palsy and Ocular Factors for Predicting Prognosis", Korean Journal of Ophthalmology, 2022

 Crossref
- Gumuyang Zhang, Lili Xu, Lun Zhao, Li Mao, Xiuli Li, Zhengyu Jin, Hao Sun. "CT-based radiomics to predict the pathological grade of bladder cancer", European Radiology, 2020 Crossref
- Cheng Dong, Ying-mei Zheng, Jian Li, Zeng-jie Wu, $_{20 \text{ words}} < 1\%$ Zhi-tao Yang, Xiao-li Li, Wen-jian Xu, Da-peng Hao. "A CT-based radiomics nomogram for differentiation of squamous cell carcinoma and non-Hodgkin's lymphoma of the palatine tonsil", European Radiology, 2021 $_{\text{Crossref}}$
- www.pubfacts.com
 19 words < 1 %
- Hejing Wang, Xiaojin Li, Donghu Zhou, Jian Huang. 17 words <1% "Autoantibodies as biomarkers for colorectal cancer: A systematic review, meta-analysis, and bioinformatics analysis", The International Journal of Biological Markers, 2019 Crossref
- Jooae Choe, Sang Min Lee, Kyung-Hyun Do, Seonok Kim, Sehoon Choi, June-Goo Lee, Joon Beom Seo. "Outcome prediction in resectable lung adenocarcinoma patients: value of CT radiomics", European Radiology, 2020

- www.e-sciencecentral.org $\frac{15}{16}$ words $-\frac{1}{9}$
- medicine-greece.blogspot.com 14 words < 1%
- Yumei Jin, Mou Li, Yali Zhao, Chencui Huang, Siyun Liu, Shengmei Liu, Min Wu, Bin Song. 13 words <1% "Computed Tomography-Based Radiomics for Preoperative Prediction of Tumor Deposits in Rectal Cancer", Frontiers in Oncology, 2021 Crossref
- 18 apo.org.au $_{\text{Internet}}$ 13 words -<1%
- cancerimagingjournal.Biomedcentral.Com 13 words < 1%
- Mudan zhang, Xuntao Yin, Wuchao Li, Yan Zha, Xianchun Zeng, Xiaoyong Zhang, Jingjing Cui, Zhong Xue, Rongpin Wang, Chen Liu. "Value of Radiomics Features From Adrenal Gland and Periadrenal Fat in CT Images for Predicting COVID-19 Prognosis", Research Square Platform LLC, 2021

 Crossref Posted Content

- 21 www.mdpi.com 11 words < 1%
- Xing Tang, Haolin Huang, Peng Du, Hong Yin, Xiaopan Xu. "Intratumoral and Peritumoral CT-Based Radiomics Strategy Reveals Distinct Subtypes of Nonsmall-Cell Lung Cancer", Research Square Platform LLC, 2021

pdfs.semanticscholar.org	10 words — < 1 %
24 www.fightmalnutrition.eu	10 words — < 1 %
25 www.science.gov Internet	10 words — < 1%
journals.lww.com Internet	9 words — < 1%

- Heba F. Pasha, Mohamed I. Radwan, Ahmed M. Yehia, Mostafa M. Toam. "Circulating methylated RUNX3 and SFRP1 genes as a noninvasive panel for early detection of colorectal cancer", European Journal of Gastroenterology & Hepatology, 2019

 Crossref
- Honglin Bai, Wei Xia, Xuefu Ji, Dong He, Xingyu Zhao, Jie Bao, Jian Zhou, Xuedong Wei, Yuhua Huang, Qiong Li, Xin Gao. "Multiparametric Magnetic Resonance Imaging Based Peritumoral Radiomics for Preoperative Prediction of the Presence of Extracapsular Extension With Prostate Cancer", Journal of Magnetic Resonance Imaging, 2021

Lin-lin Tong, Peng Gao, Zhen-ning Wang, Yong-xi Song, Ying-ying Xu, Zhe Sun, Cheng-zhong Xing, Hui-mian Xu. "Is the Seventh Edition of the UICC/AJCC TNM Staging System Reasonable for Patients With Tumor Deposits in Colorectal Cancer?", Annals of Surgery, 2012 Crossref



Lihu Gu, Ping Chen, Hui Su, Xinlong Li, Hepan Zhu, 7 words — < 1% Xianfa Wang, Parikshit Asutosh Khadaroo, Danyi Mao, Manman Chen. "Clinical Significance of Tumor Deposits in Gastric Cancer: a Retrospective and Propensity Score-Matched Study at Two Institutions", Journal of Gastrointestinal Surgery, 2019

Crossref

OFF

EXCLUDE BIBLIOGRAPHY OFF EXCLUDE MATCHES OFF

OFF